Maneuver detection of space objects using Generative Adversarial Networks

R. Abay, S. Gehly, S. Balage, M. Brown and R. Boyce
School of Engineering and IT, UNSW Canberra Space, Canberra, Australia

ABSTRACT

Maneuver detection and characterization in near-real time are helpful for identifying anomalous orbital behavior and associated threats, such as close approaches, to the neighboring space assets. In addition, such capability facilitates the maintenance of space object catalogs reducing the workload that is necessary for recapturing the lost objects between observations. Although there are studies that investigate the feasibility of detecting and characterizing maneuvers from observations, they are compute-intensive. This paper presents a deep generative model that can learn the normal orbital behavior of resident space objects and detect maneuvers in near-real-time (NRT). The input data are simulated orbital evolutions, with a high fidelity force and realistic space environment modeling, to represent the distribution that is similar to real observations. Because the success of machine learning methods depends on the representation of the input data, the simulated orbital trajectories are represented in various orbital elements, such as, specific energy, angular momentum, and equinoctial elements, to find the most appropriate form that improves the learning of the neural networks. This work investigates the feasibility of using the Generative Adversarial Network (GAN) to detect the maneuvers conducted by space objects. The generative model can recover complex high dimensional distribution of the normal orbital behavior. Therefore, any unexpected orbital evolution can be detected. The results show that GANs can learn the normal behavior of the resident space object under natural forces and detect maneuvers as anomalies.

1 INTRODUCTION

There are over 20000 resident space objects with a size larger than a softball that are being tracked and cataloged [1]. Affordability and accessibility of space with new launch providers and companies supplying low-cost hardware will drastically increase the number of objects to be tracked. Therefore, space surveillance sensors and associated algorithms that support the space situational awareness operations need to be improved accordingly. Efficient methods regarding the association of observations and maneuver detection are essential to catalog the objects accurately.

Maneuver detection of resident space objects from observational data is investigated extensively in the literature. The attention of interest is shifted from human-based analyses [2] to automated methods that require less or no human intervention [3]. Optimal control-distance metric and associated control-distance distributions, which assumes that maneuvers were fuel-efficient, were used to detect and characterize the maneuvers [4, 5]. A binary hypothesis test was applied to the control-cost probability density functions (PDFs) to predict the probability of a maneuver [5].

Admissible region method was widely used to correlate observation tracklets by imposing constraints on the states that were not directly observable [6, 7]. The object correlation and tracking problem were also studied by finite-set statistics with an adaptive Gaussian mixture model that accounts for the propagation of the multi-object uncertainty [8]. Kelecy and Jah applied batch least squares (BLSQ) and extended Kalman Filter (EKF) to detect single low-thrust in-track maneuvers (cm/s) [29]. In addition, a few recent studies applied machine learning methods, such as discriminative models and reinforcement learning, to detect and characterize the maneuvers. Linares and Furfaro used inverse reinforcement learning to estimate the reward function that was used to control the spacecraft assuming that the trajectories were optimal regarding the reward function [9]. Shabarekh et al. applied similarity-based clustering and Support Vector Machine (SVM) to predict future maneuvers of a GEO spacecraft by learning the historical pattern of its maneuvers [3, 10]. Singh et al. developed an end-to-end machine learning model that detects anomalies using principal component analysis method and characterized the detected objects using supervised learning based on observed light curves [11].

This paper investigates the feasibility of using Generative Adversarial Networks (GANs) [12] to detect maneuvers as anomalies after learning the probability distribution of normal behavior for a GEO spacecraft. In this context, the normal behavior is natural dynamics under space environmental interactions while the anomalies are the maneuvers. Anomaly detection problem was extensively studied in different domains, such as network security [13], industrial monitoring [14], video surveillance [15], and remote sensing [16]. A few recent studies applied GANs to detect anomalies by learning the normal behavior as GANs can represent complex and high dimensional distributions [17, 18]. Schlegl et al. developed the first anomaly detection GAN that can detect anomalies in the retinal images without any labeled data [19]. Zenati et al. improved the efficiency of the

Copyright © 2018 Advanced Maui Optical and Space Surveillance Technologies Conference (AMOS) – www.amostech.com

method mentioned above by training an encoder that learns to map samples to latent space, which is the space where similar features should be clustered together, simultaneously during the regular adversarial training scheme of GANs [20, 21]. This work uses a GAN architecture that is similar to the one in the Zenati's work.

In the present work, a Bidirectional Generative Adversarial Network (BIGAN) [20], which can model the manifold representation of the normal orbital behavior of a GEO object between two points in time, is used to detect maneuvers. The training data are the differences in orbital energy, angular momentum and angle states that define the orbits between two points in time. A Gaussian mixture model representation of the initial conditions of a representative GEO object (Optus 10) using five years of two-line elements history is computed [22]. The position vector is derived from sampled latitude, longitude, altitude. The velocity vector is computed by solving constraint optimization. The constraints enforce velocity to satisfy the sampled inclination and the flight path angle of 0 at epoch time. The orbits are propagated by high fidelity numerical orbit propagator which includes precise time and frame transformations [23]. The angle states are some equinoctial and Keplerian orbital elements, namely eccentricity, inclination, Ex, Ey. Keplerian mean motion is also a part of 9 feature vectors. Feature vectors are chosen based on their significance in the difference when a maneuver is executed. The total number of labeled training data (1D) that includes normal orbital state mappings between two points in time is 100000. The test data are not used during the adversarial training, and they include 14040 samples, half of which are the normal behavior samples. The results show that the trained BIGAN is capable of detecting maneuvers (m/s) between two points in time by computing the anomaly score based on the sample-to-latent space mapping loss function [19]. The variation in time will be added as another dimension to the feature vectors in the future works.

The paper is structured as follows: In section 2, the methods for creating feature vectors to train and test the BIGAN is introduced. In section 3, an overview of relevant GAN architectures are explained, and the theory regarding anomaly detection using GANs is presented. In section 4, the performance of the trained BIGAN in detecting maneuvers is provided. In section 5, the conclusions and future works based on the results are discussed.

2 DATA GENERATION

2.1 Gaussian Mixture Model for Initial Conditions

The training and test data for BIGAN are created using a high fidelity orbit propagator [23]. Because BIGAN learns the manifold representation of the normal orbital behavior between two points in time, the initial conditions should be representative of the probable orbital states of a GEO spacecraft. Although the intention is not learning the normal behavior of a specific object, Optus 10 GEO satellite is chosen due to the convenience of its location for possible future optical surveys. TLEs of Optus 10 over five years are obtained from the official space catalog [24]. There are approximately 2000 initial condition sets, and this is not enough to train BIGAN efficiently to learn the normal behavior between two points in time. A Gaussian mixture model consisting of dimensions latitude, longitude, altitude, eccentricity, and inclination to sample more initial conditions is computed.

$$\begin{aligned} &Objective\ Function: && \frac{\vec{r}\times\vec{v}}{|\vec{r}\times\vec{v}|}[0\ 0\ 1] = cos(i) \\ &\text{Constraint \# 1} && : \quad |\vec{v}| = v_{sampled} \\ &\text{Constraint \#2} && : \quad \vec{r}\cdot\vec{v} = 0 \end{aligned} \tag{1}$$

In Fig. 1, the density plots for latitude, longitude, altitude, eccentricity and inclination histories of the Optus 10 satellite over five years is shown. Although the initial conditions are modeled using a Gaussian mixture model to sample many initial conditions to compute training and test data by propagating them forward in time, the propagation of the available initial conditions for creating more initial conditions is a better approach if a specific spacecraft behavior is intended to be learned. The velocity vector should be computed by solving the constraint optimization problem that satisfies the sampled inclination and eccentricity for the Gaussian mixture model approach. Eq. 1 shows the objective function, which satisfies inclination (i), and two constraints to compute the velocity vector after the inertial position vector in J2000 reference frame is computed from sampled latitude, longitude and altitude. After the position vector is defined, the magnitude of the associated velocity vector ($v_{sampled}$) is computed using the sampled eccentricity and corresponding semi-major axis. The objective function is solved assuming that the spacecraft is at its perigee. The approach mentioned above tends to compute

Copyright © 2018 Advanced Maui Optical and Space Surveillance Technologies Conference (AMOS) – www.amostech.com

lower eccentric orbit than sampled eccentricity, and this makes it less favorable if a normal behavior of a specific spacecraft is intended to be learned.

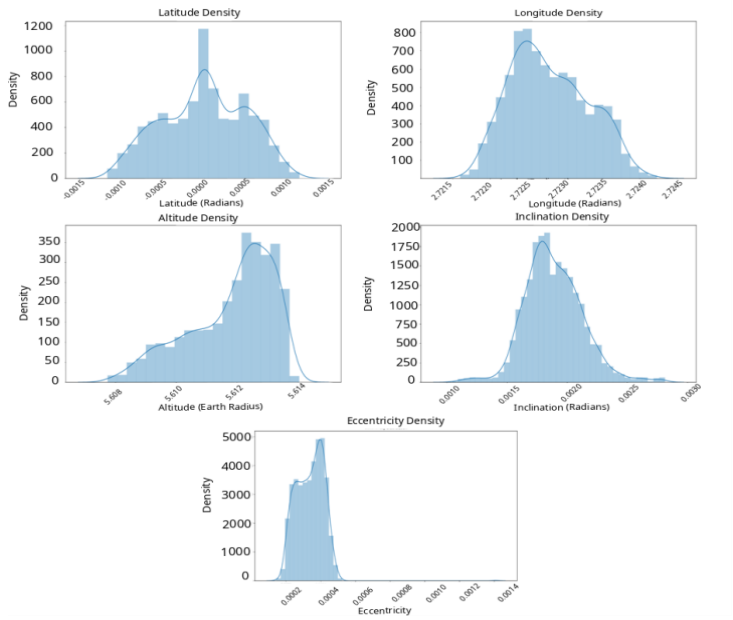

Fig.1. Density plots of initial latitude, longitude, altitude, eccentricity and inclination of Optus 10 satellite.

2.2 Feature Vectors

The training data includes the orbital evolution of the spacecraft under natural space environment forces and the associated target label that is normal. The propagation time is chosen as 14 hours for this paper. Because maneuvers change the state of orbit, namely specific energy, angular momentum, and orbital angles, the feature vectors are selected accordingly. In addition to the energy and angular momentum of the orbit, Keplerian mean motion, eccentricity, inclination; Equinoctial Ex and Ey are selected as feature vectors. Table 1 shows the differences in the feature vectors within 14 hours. In future work, the time difference will be added to the feature vectors and the normal behavior in any time difference for the spacecraft will be learned. The focus of this effort is to investigate the sensitivity of the proposed approach to the magnitude and direction of the maneuvers. In Fig. 2, the normal and maneuver cases are presented.

Table 1. The feature vectors

Features	Explanations ($t_0 = 0\ h, t_f = 14\ h$)	Equations [25]
$\Delta\varepsilon$	Difference between specific mechanical energies	$\varepsilon = \frac{v^2}{2} - \frac{\mu}{r}$
$\Delta\lvert\vec{H}\rvert$	Difference between the magnitudes of orbital angular momentums	$\vec{H} = \vec{r}x\vec{v}$
$\Delta\frac{\vec{H}}{\lvert\vec{H}\rvert}$	Cosine of the complementary angle between orbital angular momentum directions	$\vec{H} = \vec{r}x\vec{v}$
Δh	Difference between the magnitudes of specific angular momentums	$h = \sqrt{\mu a(1-e^2)}$
Δn	Difference between mean motions	$n = \sqrt{\frac{\mu}{a^3}}$
Δe	Difference between eccentricities	$e = \frac{a - r_p}{a}$
Δi	Difference between inclinations	$i = \mathrm{acos}(\frac{\vec{K}\vec{H}}{\lvert\vec{K}\vec{H}\rvert})$
ΔEx	Difference between equinoctial Ex parameters	$E_X = e\cos(\omega + \Omega)$
ΔEy	Difference between equinoctial Ey parameters	$E_y = e\sin(\omega + \Omega)$

Copyright © 2018 Advanced Maui Optical and Space Surveillance Technologies Conference (AMOS) – www.amostech.com

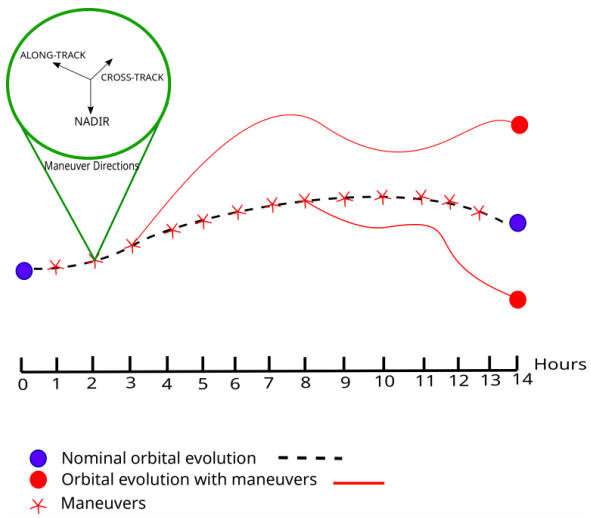

Fig. 2. The normal and maneuver cases.

3 GENERATIVE ADVERSARIAL NETWORKS

3.1 Generative Adversarial Network

Discriminative machine learning methods, such as neural networks, support vector machines, and decision trees, determines the boundary between classes, while generative machine learning models model the classes, therefore, it can generate samples. Generative Adversarial Network is a promising machine learning method invented in 2014 [12]. It is based on training two neural networks in an adversarial framework to extract the input data distribution. Its implementation is quite difficult because the conventional approach to train a single neural network does not work directly on GANs. One of the neural networks of GANs is called the generator, and the other one is called the discriminator. Both models play a zero-sum game to reach the Nash equilibrium [26]. The generator tries to capture the underlying data distribution of the input data to deceive the discriminator, whereas the discriminator attempts to detect whether the presented sample comes from real data or created by the generator. The discriminator is a binary classifier which determines input data to be either fake (generated by the generator) or real (the input data). Fig. 3 shows the GAN architecture. The adversarial objective function is shown in Eq. 2 [12]. The first part of the objective function enforces the discriminator to predict 1 for the real samples, while the second part enforces it to predict 0 for the ones that are generated by the generator. The generator creates realistic samples from the latent space (z). Both the discriminator and generator are differentiable neural network architectures, and they can be learned by gradient descent method.

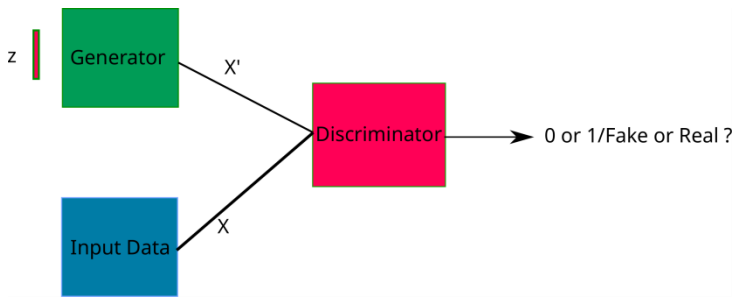

Fig. 3. The Generative Adversarial Network architecture.

$$Objective\ Function: \quad E_{x\sim p_x}[\log D(x)] + E_{z\sim p_z}[\log(1 - D(G(z)))] \tag{2}$$

Fig. 4 shows generative models that perform maximum likelihood. GANs do not represent the data density in an explicit form, however, through its adversarial training framework they can generate it. Generally, it is intractable to represent the data density. Variational autoencoders and Boltzmann machines suffer from approximating the explicit density functions [27]. Implicit methods samples from the data distribution without explicitly defining it. Generative Stochastic Network (GSN) uses a computationally intensive Markov chain to

Copyright © 2018 Advanced Maui Optical and Space Surveillance Technologies Conference (AMOS) – www.amostech.com

sample from a distribution. However, GANs can directly sample high dimensional complex data without the need for representing the density function [27].

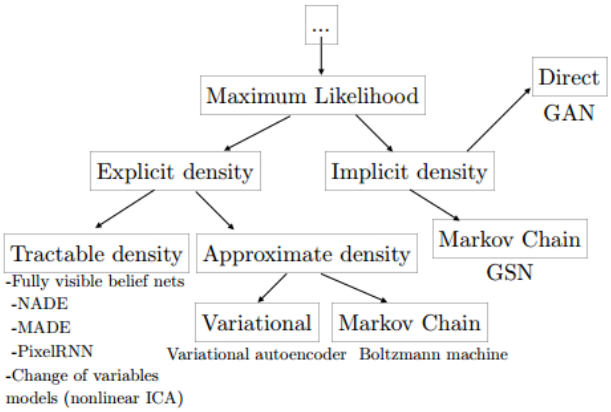

Fig. 4. The generative machine learning models [27].

3.2 Maneuver detection with Bidirectional Generative Adversarial Network

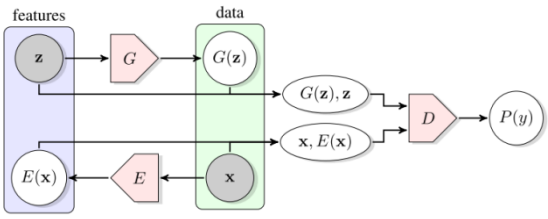

Fig. 5. The architecture of BIGAN [28].

The standard GAN can map from latent space (z) to data (x), yet it cannot do the inverse. Such capability is essential to anomaly detection applications because the capability to conduct bidirectional mapping leads to a score function that determines the distance between the given sample and the corresponding sample generated from the latent space (z). In addition, the anomaly detection becomes computationally efficient at test time when such a model is trained along with the generative and discriminative models [21]. Therefore, an encoder E, which can map data x to latent space z, is trained simultaneously during the adversarial training [28]. Fig. 5 shows the architecture of the BIGAN. In this work, the adversarial training of encoder E [28] and the score function for determining the anomalous samples [19] are implemented similar to the architecture presented in Zenati's paper [21]. Because an encoder that can map from x to z such that $E = G^{-1}$ is essential to anomaly detection, the objective function for adversarial training is defined as in Eq. 3.

$$Objective\ Function: \ E_{x\sim p_x}\left[E_{x\sim p_E(.|x)}[\log D(x,z)]\right] + E_{z\sim p_z}[E_{x\sim p_G(.|z)}[\log(1 - D(G(z)))]] \tag{3}$$

Where $p_X(x)$ is data distribution, $p_Z(z)$ is latent space distribution, $p_E(z|x)$ and $p_G(x|z)$ are the distributions generated by the encoder and generator respectively. In a nutshell, the encoder that can map a sample from data (x) distribution to the latent space distribution (z) is needed to detect anomalies to the normal behavior learned by adversarial training. A score function that can detect the anomalies to the expected behavior using the generator, encoder and discriminator models can be defined as in Eq. 4 which includes losses associated with the generator and discriminator [19].

$$A(x) = \alpha \parallel x - G(E(x)) \parallel_1 + (1-\alpha) \parallel f_D(x, E(x)) - f_D(G(E(x)), E(x)) \parallel_1 \tag{4}$$

Where f_D is a function that outputs the layer before the logits in the discriminator for a given input, and this determines whether the generated data have features similar to the true sample in the discriminator or not. This approach is called a feature-matching method [19]. Larger values of the function $A(x)$ indicate that the sample is anomalous. The present architecture of the model for maneuver detection is shown in Fig. 6. The hyper-parameters for the neural networks are provided in Table 2 [21].

Copyright © 2018 Advanced Maui Optical and Space Surveillance Technologies Conference (AMOS) – www.amostech.com

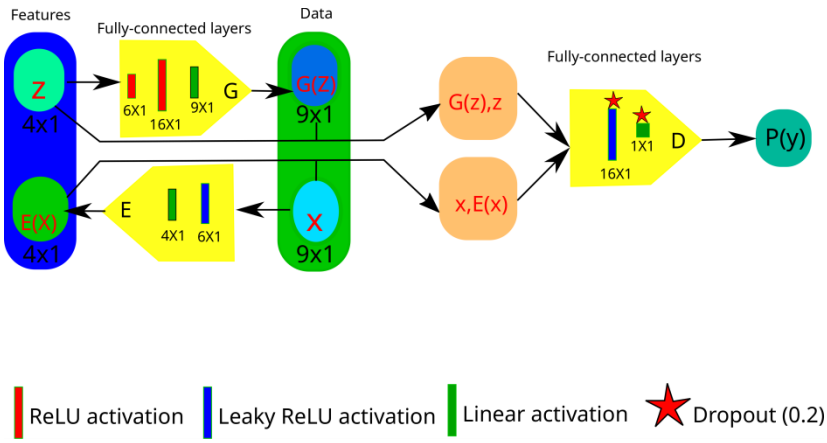

Fig. 6. The architecture of BIGAN for maneuver detection.

Table 2. The hyper-parameters of maneuver detection BIGAN

Parameters	Values
Optimizer	Adam optimizer ($\alpha = 1e-5, \beta_1 = 0.5$)
Batch size	50
Latent dimension	4
Epochs	10
Leaky ReLU slope	0.1
Weight initialization	Xavier initializer
Bias initialization	0

4 RESULTS

The BIGAN that is trained to detect maneuvers as anomalies between two points in time is implemented. The precision is 100%, recall is 94%, and F1 score is 97%. The equations for precision, recall and F1 score are presented in Eq. 5. The false negatives that are responsible for lower recall compared to precision indicate that the model has some difficulty in distinguishing maneuvers from normal orbital evolution for some orbits and maneuvers. In Fig. 7, the percentage errors of the applied maneuvers that contribute to false negatives are shown. The results indicate that the performance of BIGAN can be improved by adding additional feature vectors that capture the change regarding the true anomaly. It can be seen that maneuvers with small magnitudes applied closer to the epoch yield less information about the difference between two orbital states. As there are no feature vectors that can give information regarding the location of the space object in orbit directly, the relatively poor performance is expected. The maneuvers conducted close to the second observation time in the cross-track and nadir directions create small changes to the feature vectors. Therefore, additional feature vectors that can capture the change between two orbital states within a shorter period of time should be added to improve BIGAN further.

$$\begin{aligned} Precision &: \frac{True\ Positive}{True\ Positive + False\ Positive} \\ \text{Recall} &: \frac{True\ Positive}{True\ Positive + False\ Negative} \\ \text{F1} &: 2\frac{Precision \cdot Recall}{Precision + Recall} \end{aligned} \tag{5}$$

Copyright © 2018 Advanced Maui Optical and Space Surveillance Technologies Conference (AMOS) – www.amostech.com

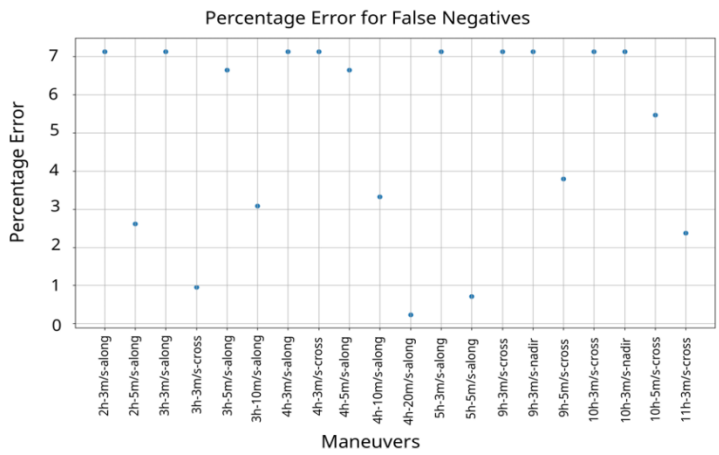

Fig. 7. The percentage error of maneuvers applied to the false negatives.

5 CONCLUSIONS AND FUTURE WORK

The feasibility of detecting maneuvers between two points in time is investigated using Bidirectional Generative Adversarial Networks. BIGAN is a type of GAN that can map data (x) to the latent space (z) using an encoder in addition to the standard capability of mapping from z to x using the generator. The loss function used to train the encoder tries to minimize the error between E(x) and z which is not only helpful to increase the testing speed drastically but also learning the location of x in the latent space. The capability of knowing the manifold representation of x is essential for anomaly detection applications. In this work, normal orbit behavior under space environment interactions, namely Earth's aspherical gravitational potential, third-body mass, and solar radiation pressure, is learned and any anomaly is detected as maneuvers.

First, the initial orbit parameters are computed using a GEO satellite (Optus 10), and a Gaussian mixture model is computed from them. Because it is not intended to learn the normal behavior of a specific object, this approach is effective since once the GMM is computed many samples can be obtained from it. Then, the inertial position vector in the J2000 reference frame is computed from sampled latitude, longitude and altitude. After that, the velocity vector is computed from sampled eccentricity and inclination using an equality constraint optimization problem (Eq. 1). Next, feature vectors that are the difference of two orbital states at two points in time (14 hours) are computed. There are 100000 training data samples for the normal behavior, and 14040 data samples, half of which are of normal behavior are chosen as test data. Finally, a BIGAN is modeled with training data and tested using the test data which are not used during the training.

The initial results, the precision of 100%, recall of 94% and the F1 score of 97%, are promising. The focus of this work is to understand the sensitivity of maneuvers on BIGAN to detect them and improve feature vectors to capture subtle changes in the orbital states when the maneuvers are applied. Therefore, a fixed 14-hour duration is chosen as the time period between two observations. An additional orbit angle information could further improve the results. The maneuvers with small magnitudes in the along-track direction close to the first observation and the small maneuvers in the nadir and cross-track directions close to the second observation time lead to false positives. Once the features vectors are revised to improve the performance of the BIGAN further, the time will be added as another dimension to have a model that can sample orbital state difference of a GEO object in any time periods. Because the normal behavior of an object is learned through sampling, uncertainty can easily be managed by coupling all samples within the covariance at the two points in time.

6 REFERENCES

1. National Aeronautics and Space Administration (NASA). Last accessed 08/29/2018. https://www.nasa.gov/mission_pages/station/news/orbital_debris.html
2. Hoots, F. R., Schumacher, P. W., "History of Analytical Orbit Modeling in the U.S. Space Surveillance System," Journal of Guidance, Control, and Dynamics, Vol. 27, No. 2, 2004, pp. 174–185. https://doi.org/10.2514/1.9161
3. Shabarekh C., Kent-Bryant J., Garbus M., Keselman G., Baldwin J., Engberg B., "Efficient Object Maneuver Characterization For Space Situational Awareness", 32nd Space Symposium, Technical Track, Colorado Springs , Colorado, United States of America. Presented on April 11-12, 2016.

Copyright © 2018 Advanced Maui Optical and Space Surveillance Technologies Conference (AMOS) – www.amostech.com

4. Holzinger, M. J., Scheeres, D. J., and Alfriend, K. T., "Object Correlation, Maneuver Detection, and Characterization Using Control- Distance Metrics," Journal of Guidance, Control, and Dynamics, Vol. 35, No. 4, July 2012, pp. 1312–1325. doi:10.2514/1.53245. https://doi.org/10.2514/1.53245
5. Andris D. Jaunzemis, Midhun V. Mathew, and Marcus J. Holzinger. "Control Cost and Mahalanobis Distance Binary Hypothesis Testing for Spacecraft Maneuver Detection", Journal of Guidance, Control, and Dynamics, Vol. 39, No. 9 (2016), pp. 2058-2072. https://doi.org/10.2514/1.G001616
6. Tommei, G., Milani, A., and Rossi, A., "Orbit Determination of Space Debris: Admissible Regions," Celestial Mechanics and Dynamical Astronomy, Vol. 97, No. 4, 2007, pp. 289–304. https://doi.org/10.1007/s10569-007-9065-x
7. Maruskin, J. M., Scheeres, D. J., and Alfriend, K. T., "Correlation of Optical Observations of Objects in Earth Orbit," Journal of Guidance, Control, and Dynamics, Vol. 32, No. 1, Jan. 2009, pp. 194–209. https://doi.org/10.2514/1.36398
8. DeMars, K. J., Hussein, I. I., Frueh, C., Jah, M. K., and Scott Erwin, R., "Multiple-Object Space Surveillance Tracking Using Finite-Set Statistics," Journal of Guidance, Control, and Dynamics, Vol. 38, No. 9, March 2015, pp. 1741–1756 . https://doi.org/10.2514/1.G000987
9. Linares R., Furfaro R., "Space Objects Maneuvering Detection and Prediction via Inverse Reinforcement Learning", Proceedings of the Advanced Maui Optical and Space Surveillance (AMOS) Technologies Conference, held in Maui, Hawaii, September 19-22, 2017.
10. Shabarekh C., Kent-Bryant J., Keselman G., Mitidis A., "Space Objects Maneuvering Detection and Prediction via Inverse Reinforcement Learning", Proceedings of the Advanced Maui Optical and Space Surveillance Technologies Conference, held in Maui, Hawaii, September 20-23, 2016.
11. Singh N., Horwood J. T., Aristoff J. M., Murray- Krezan J., "Athena: a data-driven anomaly detection and space object classification tool for SSA," in Proceedings of the 26th AAS/AIAA Space Flight Mechanics Meeting, Napa, CA, February 2016 (Paper AAS-16-447)
12. Goodfellow I., Pouget-Abadie J., Mirza M., Xu B., Warde-Farley D., Ozair S., Courville A., Bengio Y. "Generative adversarial nets". Advances in Neural Information Processing Systems, pp. 2672–2680, 2014.
13. Jyothsna V., Prasad V.V. R., Prasad K.M. "A review of anomaly based intrusion detection systems. International Journal of Computer Applications", 28(7):26–35, 2011. https://doi.org/10.5120/3399-4730
14. Clifton D.A., Bannister P.R., Tarassenko L., "Learning shape for jet engine novelty detection". International Symposium on Neural Networks, pages 828–835. Springer, 2006.
15. Pokrajac D., Lazarevic A., Latecki L.J., "Incremental local outlier detection for data streams". Presented at IEEE Symposium on Computational Intelligence and Data Mining, pages 504–515. IEEE, 2007.
16. Matteoli, S., Diani, M., Theiler, J.: An overview of background modeling for detection of targets and anomalies in hyperspectral remotely sensed imagery. IEEE Journal of Selected Topics in Applied Earth Observations and Remote Sensing 7(6) (2014) 2317–2336. https://doi.org/10.1109/JSTARS.2014.2315772
17. Radford A., Metz L., Chintala S. "Unsupervised representation learning with deep convolutional generative adversarial networks". Presented at International Conference on Learning Representations, Workshop Track, 2016.
18. Creswell A., White T., Dumoulin V., Arulkumaran K., Sengupta B., Bharath A.A. "Generative adversarial networks: An overview". Proceedings of IEEE Signal Processing Magazine Special Issue on Deep Learning for Visual Understanding, 2017.
19. Schlegl T., Seebock P., Waldstein S.M., Schmidt-Erfurth U., Langs G. "Unsupervised anomaly detection with generative adversarial networks to guide marker discovery". Presented at International Conference on Information Processing in Medical Imaging, pages 146–157. Springer, 2017.
20. Poole B., Lamb A., Arjovsky M., Mastropietro O., Dumoulin V., Belghazi I., Courville A. "Adversarially learned inference". Presented at International Conference on Learning Representations, 2017.
21. Zenati H., Foo C.S., Lecouat B., Manek G., Chandrasekhar V.R. "Efficient GAN-based anomaly detection". arXiv preprint arXiv:1802.06222, 2018.
22. Joint Space Operations Center (JSpOC). Last accessed 2018/07/25. https://www.space-track.org/
23. Abay R., Gehly S., Brown M., Boyce R., High Area-To-Mass Ratio Object Characterization Using Machine Learning. *42nd COSPAR Scientific Assembly*, Pasadena, California, 14-22 July 2018.
24. Joint Space Operations Center (JSpOC). Last accessed 2018/08/01. https://www.space-track.org
25. Vallado D. A. "Fundamentals of Astrodynamics and Applications". McGraw-Hill Companies, Inc., 1997.
26. Nash J.F. "Equilibrium points in N-person games". Proceedings of the National Academy of Sciences of the United States of America, 36, 1950.
27. Goodfellow I. Generative Adversarial Networks (NIPS 2016 tutorial), 2016.
28. Donahue J., Krähenbühl P., Darrell T. "Adversarial feature learning". Published as a conference paper at ICLR 2017, 2017.
29. Kelecy, T., and Jah, M., "Detection and Orbit Determination of a Satellite Executing Low Thrust Maneuvers," Acta Astronautica, Vol. 66, No. 5, 2010, pp. 798–809.

Copyright © 2018 Advanced Maui Optical and Space Surveillance Technologies Conference (AMOS) – www.amostech.com